Prolonged Irradiation-induced Delayed Luminescence of Imide Compounds Dispersed in Polymer Matrix and its Relation to Oxygen Quenching

Marina DOI, Ryohei ISHIGE, Shinji ANDO

Dept. Chemistry and Materials Science, Tokyo Institute of Technology,
Ookayama 2-12-1-E4-5, Meguro-ku, Tokyo, 152-8552, Japan
E-mail: doi.m.aj@m.titech.ac.jp

Long-lived room-temperature delayed phosphorescence, called prolonged irradiation-induced delayed luminescence (PIDL), was observed in air for three imide compounds (ICs) dispersed in poly(methyl methacrylate) under UV irradiation after an induction time of 1.60–6.78 min, whereas the ICs showed only fluorescence after a short period of UV irradiation. The induction time until the appearance of PIDL was linearly proportional to the oxygen concentration. The PIDL emission continued as an afterglow for several seconds (0.36–1.30 s) after the irradiation was stopped. The generation mechanism of PIDL was investigated and clarified based on the optical measurements and numerical simulation. This study demonstrates that the PIDL phenomenon is essentially based on the oxygen quenching, which is energy transfer from excited triplet state of ICs to ground state triplet oxygen, indicating that PIDL can be applied to the molecular design of new categories of Long-lived room-temperature materials.

1. Introduction

Long-lived luminescent (LL) materials have attracted significant attention because of their long luminescence lifetime for several seconds to more than 10 hours upon exposure to external stimuli, such as heat, tensile stress, pressure, light, or electricity.[1–3] These LL materials have been applied in various fields, including bio-imaging,[4] information security,[5] glow-in-the-dark paints,[6] and emergency signs.[6] Most LL materials used in commercial applications are inorganic crystals, such as $CaAl_2O_4$ and $SrAl_2O_4$. However, they are environmentally hazardous and toxic, requiring high-temperature processes exceeding 1000 °C. LL materials made of organic compounds have attracted significant attention in recent years because of their simple process, excellent flexibility and formability, and non-toxicity. Therefore, many organic LL materials have been studied. However, their luminescence lifetimes are extremely short compared with those of inorganic LL materials.

One of the luminescence of organic compounds studied as LL is phosphorescence (PH).[7] The PH of organic molecules has a wide range of luminescence lifetimes of 10^{-6}–10 s. However, room-temperature PH (RTP) is rarely observed in air because the excited triplet state (T_1) is easily deactivated by local molecular motion or excitation energy transfer to oxygen in the material or air. A pure organic LL-PH observable at room temperature in air is desirable for environmentally friendly applications. Therefore, two main strategies for developing LL-PH materials have been studied. One is to increase the rate constant of the intersystem crossing (ISC) and the other is to suppress non-radiative deactivation from T_1. For the former, the ISC can be enhanced using the heavy atom effect. RTP has been realized by introducing heavy metals or halogens, such as iridium, Cl, and Br, into luminescent polymer materials.[8–11] For the latter, crystallization,[12,13] molecular aggregation,[14,15] and host-guest systems[16,17] have been used to suppress molecular motion and oxygen quenching (OQ).

Recently, we have reported that the three types of imide compounds (ICs) dispersed in poly(methyl methacrylate) (PMMA) exhibited an intriguing delayed luminescence phenomenon at room temperature in air, known as prolonged irradiation-induced delayed luminescence (PIDL).[18] In this study, the photophysical mechanism of the PIDL was clarified based on the emission spectra measurements, the detection of singlet oxygen ($^1O_2$) during UV irradiation, and numerical simulations.

2. Experimental

The ICs, *N,N'*-dicyclohexylnaphthalene-2,3,6,7-tetracarboxylic diimide (NT-IC),[11] *N,N'*-dicyclohexylbiphenyl-3,3',4,4'-tetracarboxylic diimide (*s*BP-IC), and *N,N'*-dicyclohexyl-4,4'-oxydiphthalic imide (OD-IC), were synthesized (**Fig. 1**). The ICs and PMMA were dissolved in chloroform, and the solutions were spin-coated onto a fused silica substrate and dried at 65 °C for 1 h in *vacuo*. The weight fractions of ICs were set to 0.2 wt%.

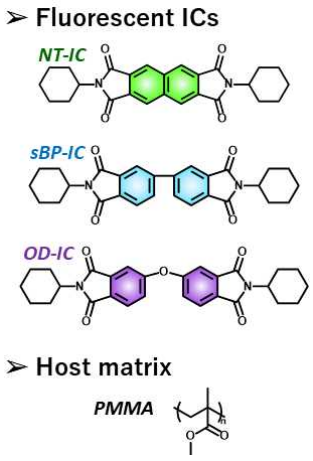

Fig. 1 Chemical structures of ICs and host matrix.

The emission spectra during UV irradiation of these films were measured using a home-made optical system and performed at every 100 ms. The PIDL decay curves after prolonged UV irradiation were plotted using the intensities of the PIDL in the emission spectra after the irradiation was stopped. Each emission spectrum was fitted using a linear combination of the FL and PIDL spectra to estimate the area ratios of these two components, and the time evolution of these peak areas was plotted against time. The emission peak areas were normalized to the FL peak area at the beginning of the UV irradiation. The emission spectra during UV irradiation under vacuum or atmospheric pressure in O_2/N_2 mixture were measured using a cell containing the films with the internal environment set to the conditions described above.

1,3-Diphenylisobenzofuran (DPBF) was used as a probe to detect the existence of $^1O_2$ by measurement of UV-vis absorption spectra. The weight fraction of ICs in the films for this measurement was set to 0.2 wt% and the molar ratio of IC:DPBF was set to 1:8. The absorption spectra were measured at every 100 ms during UV irradiation.

Numerical simulations of the PIDL process were performed using Simulink and MATLAB (MathWorks Inc., Natick, MA, USA).

3. Results and Discussion

Fig. 2 shows the time evolution of the emission spectra of NT-IC, *s*BP-IC, and OD-IC dispersed in PMMA films during continuous UV irradiation in air and under vacuum for 15 min. At the start of the irradiation, they exhibit only blue fluorescence (FL) at 384–398 nm and do not exhibit PH in air because of the quenching of the T_1 state by ambient triplet oxygen ($^3O_2$), which is called oxygen quenching (OQ). In contrast, under vacuum, they exhibit green PH at 480–510 nm in addition to FL peaks because of the absence of OQ, indicating that the T_1 state of the ICs dispersed in PMMA is sensitive to atmospheric oxygen.

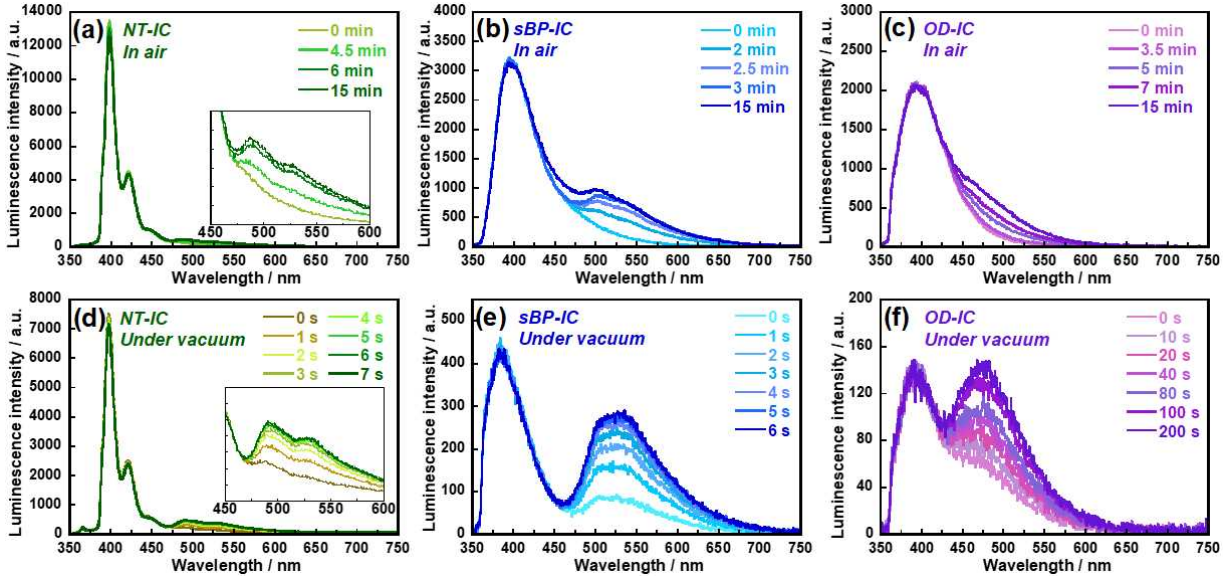

Fig. 2 Various emission spectra depending on irradiation time for (a,d) NT-IC, (b,e) *s*BP-IC, and (c,f) OD-IC dispersed in PMMA films observed in air (a–c) and under vacuum (d–f).

During prolonged UV irradiation under vacuum, the intensity of the PH gradually increased with time. This suggests that UV irradiation induced at least one of the following changes: a) an enhancement of the rate constant of ISC, b) an increase in the rate constant of PH, or c) suppression of non-radiative deactivation from the T_1 state. In contrast, in air, new emission peaks began to appear in the 450–650 nm region during prolonged UV irradiation and their intensities gradually increased with time.

Because the spectral features (wavelength ranges and shapes) of the new emissions are very close to those of the PH under vacuum, as shown in **Fig. 3**, they are readily attributable to the PH from the T_1 state. The time elapsed from the beginning of irradiation until the appearance of the new peak, which is called the "induction time," was only a few seconds under vacuum, while it was significantly longer, several minutes, in air. This suggests that oxygen is the essential factor in the delayed PH phenomenon. To distinguish the new emission from the conventional RTP observed under vacuum, we refer to it as PIDL.

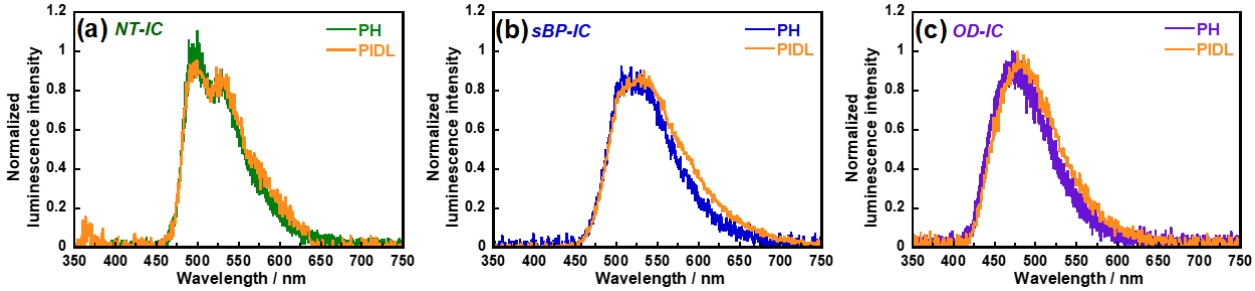

Fig. 3 Comparison of emission spectra of PIDL and PH observed under vacuum for (a) NT-IC, (b) *s*BP-IC, and (c) OD-IC dispersed in PMMA films.

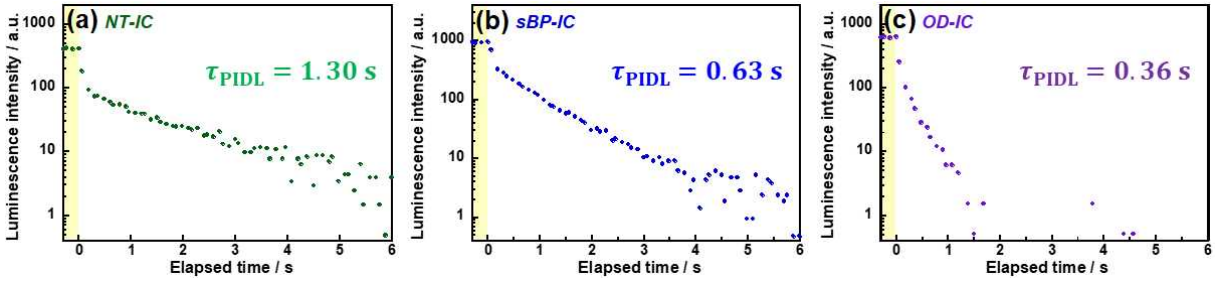

Fig. 4 PIDL decay curves for (a) NT-IC (irradiation wavelength (λ_{ir}), monitoring emission wavelength (λ_{em}) = 360, 500 nm), (b) *s*BP-IC (340, 510 nm), and (c) OD-IC (340, 480 nm) dispersed in PMMA films. The irradiation period is represented by yellow hatching.

When the UV irradiation after 15 min was stopped, a green-coloured afterglow of PIDL continued for a few seconds (**Fig. 4**), indicating that the lifetime of the PIDL (τ_{PIDL} = 0.36–1.30 s) was longer than several hundreds of msec. A typical PH lifetime (τ_p) of organic compounds is in the order of μs-ms and τ_p values longer than 100 ms are called a "long-lived PH lifetime."[19,20] Therefore, the PIDL is classified as a very long-lived PH at room temperature in air.

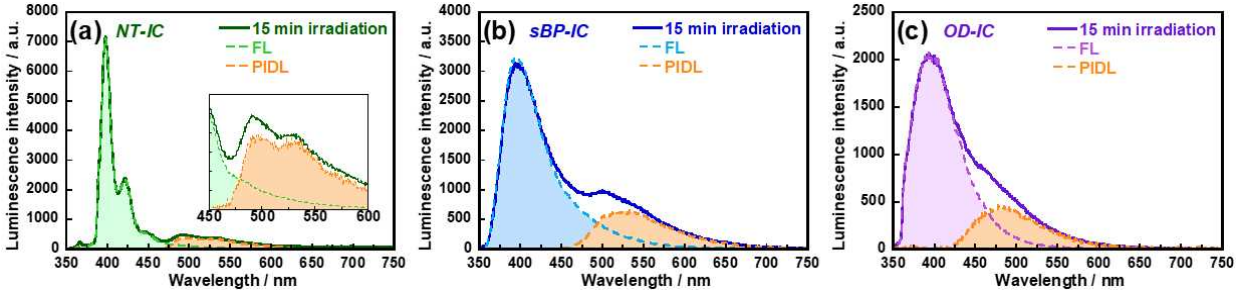

Fig. 5 Decomposed spectra into FL and PIDL (PH) components of (a) NT-IC, (b) *s*BP-IC, and (c) OD-IC dispersed in PMMA films. The emission spectra just after UV irradiation in air were chosen as FL spectra and just after the end of UV irradiation for 15 min were chosen as the PIDL spectra.

As shown in **Fig. 5**, the photoluminescence spectra observed during UV irradiation under vacuum and in air can be decomposed into two components, corresponding to FL and PIDL (or PH). **Fig. 6** shows the

irradiation-time dependence of the ratio of the integral areas of the decomposed FL and PIDL peaks under vacuum and air for NT-IC, *s*BP-IC, and OD-IC dispersed in PMMA. Under vacuum, both FL and PIDL (PH) peaks were observed just after the beginning of irradiation. Meanwhile, in air, the very long induction times (t_{ID}s), as long as several minutes (NT-IC: t_{ID}=3.83 min, *s*BP-IC: 1.60 min, OD-IC: 6.78 min), were clearly detected before the appearance of the PIDL emission. Then, the intensity of the PIDL gradually increased. This strongly suggests that the onset and growth of the PIDL are triggered and controlled by oxygen inside the PMMA films.

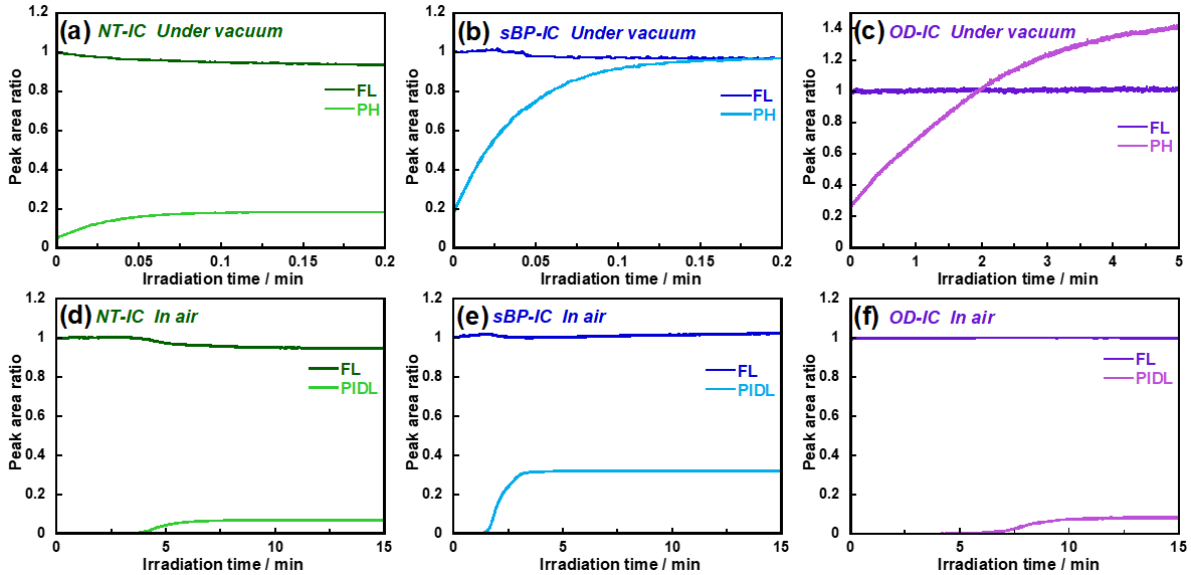

Fig. 6 Time evolution of the emission peak areas during UV irradiation (a–c) under vacuum and (d–f) in air ((a,d) NT-IC, (b,e) *s*BP-IC, (c,f) OD-IC).

Because oxygen molecules in the films affect the PIDL process of the ICs, the photophysical processes involving atmospheric oxygen should be examined. OQ is an energy-transfer phenomenon from a phosphor in the T_1 state to the surrounding $^3O_2$. In this process, $^3O_2$ is excited to the singlet state (S_n) ($^1O_2$) and the phosphor is simultaneously deactivated to the ground state (S_0).[21] Reineke *et al.*[22,23] reported that a phosphor dispersed in PMMA covered with polyvinyl alcohol (PVA) exhibited PH after prolonged UV irradiation, which could be due to the reduction in the rate constant of OQ by the consumption of $^3O_2$ *via* photodegradation of PMMA as well as the oxygen barrier performance of the PVA coating. Inspired by this report, we hypothesized that the PIDL of ICs in air is caused by the following processes, as shown in **Scheme 1**. First, at the beginning of UV irradiation in Stage (a), the excited ICs exhibited only FL without PH because PH is suppressed by OQ. Second, during the induction time in Stage (b), despite the deactivation to $^3O_2$, $^1O_2$ molecules are slowly accumulated in the excited state or consumed *via* degradation of PMMA, leading to the gradual depletion of $^3O_2$ in the ground state. Finally, when the rate constant of OQ becomes smaller than a certain threshold in Stage (c), the PH process becomes dominant and the IC molecules begin to exhibit PH, that is, PIDL. Therefore, the appearance of the PIDL is triggered by the consumption of $^3O_2$ around the ICs.

To verify the proposed PIDL mechanism, we aimed to detect $^1O_2$ generated *via* OQ when the ICs were irradiated by UV light. DPBF is a widely used

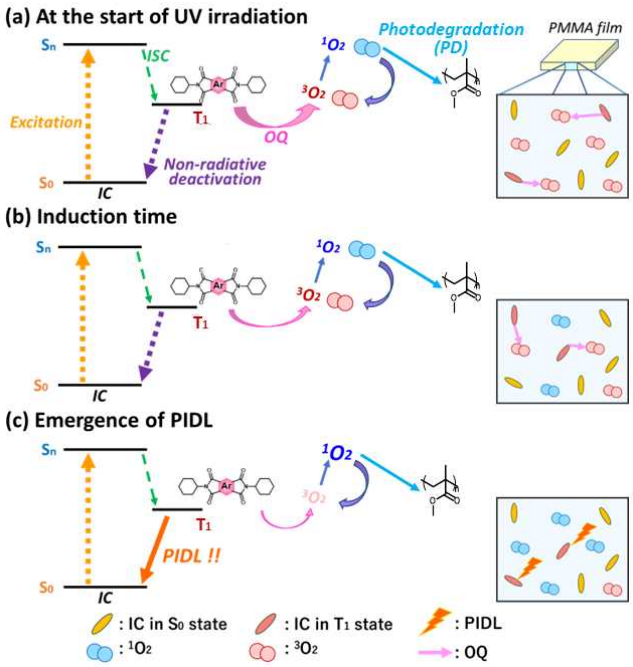

Scheme 1 Three steps of the proposed photophysical mechanism of PIDL.

probe for $^1O_2$ detection that reacts with $^1O_2$ to produce 1,2-dibenzoylbenzene (DBB).[24] DPBF has a absorption peak at 418 nm (**Fig. 7(a)**), whereas DBB does not. Therefore, the generation of $^1O_2$ can be qualitatively monitored through the time variation of the absorption peak of DPBF.[25,26] *s*BP-IC, which exhibits the strongest PIDL intensity, was used as a representative IC. PMMA film containing homogeneously dispersed both DPBF and *s*BP-IC, and a film containing only DPBF were prepared to detect $^1O_2$ and monitor the photodegradation of DPBF, respectively.

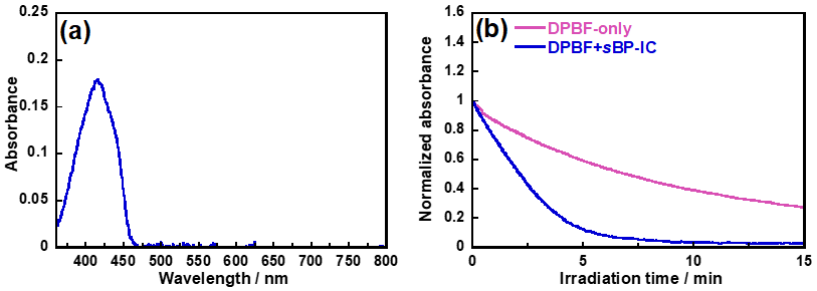

Fig. 7 (a) UV-vis absorption spectra of DPBF dispersed in PMMA film. (b) Irradiation-time dependence of the absorbance of DPBF at 418 nm for the dispersed films with DPBF only, and DPBF+*s*BP-IC in PMMA.

Fig. 7(b) shows the irradiation-time dependence of the absorbance of DPBF at 418 nm (A_{DP}). The A_{DP} of the film containing DPBF only decreased, indicating that DPBF is decomposed by UV light. In contrast, the A_{DP} in the film with DPBF and *s*BP-IC decreased much faster than that in the DPBF-only film, which strongly suggests that the $^1O_2$ generated during UV irradiation of the ICs promoted the degradation of DPBF, and support the generation mechanism of PIDL, as shown in **Scheme 1**.

To investigate the effect of oxygen concentration ($[O_2]$) outside the films on the PIDL process, PMMA films doped with ICs were placed in a silica test tube. The $[O_2]$ inside the tube was controlled between 0–27 % by mixing pure oxygen and nitrogen gases. **Fig. 8** shows the dependence of the induction time (t_{ID}) on the $[O_2]$ for NT-IC, *s*BP-IC, and OD-IC dispersed in PMMA. For all films, t_{ID} increased linearly with an increase in $[O_2]$, suggesting that the PIDL phenomenon is sensitive to $[O_2]$ in the surrounding environment.

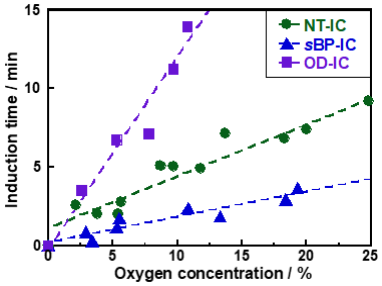

Fig. 8 O_2 concentration dependence of the induction time for ICs dispersed in PMMA.

As shown in **Fig. 8**, the slopes of the plots of t_{ID} versus $[O_2]$ decrease in the order of OD-IC>NT-IC>*s*BP-IC, which agrees well with the order of the rate constants of OQ for these ICs (NT-IC: 84300 s^{-1}, *s*BP-IC: 84700 s^{-1}, OD-IC: 83800 s^{-1}). OQ occurs *via* a Dexter-type energy transfer and the rate constant for the Dexter-type energy transfer is proportional to the integral of the overlap between the emission spectrum of the donor and the absorption spectrum of the acceptor.[21] The absorption spectrum of oxygen is in the range 580–1270 nm[27,28] and the λ_{em} of the PH of ICs is 480 nm (OD-IC), 500 nm (NT-IC), and 510 nm (*s*BP-IC). This suggests that the spectral overlap between the IC donor and oxygen acceptor increases in the order OD-IC<NT-IC<*s*BP-IC. The rate constant of OQ increases in the same order. The larger rate constant of the OQ results in a faster consumption of $^3O_2$. Therefore, $^3O_2$ decreases faster. Based on these results, because the OQ rate constant depends on the peak wavelength of PH, the PIDL materials with controlled t_{ID} can be realized by adjusting the PH wavelength of the ICs.

Numerical simulations were performed based on the PIDL mechanism shown in **Scheme 1** to verify the proposed photophysical processes. In this simulation, the concentrations of $^3O_2$ dissolved in the PMMA, ICs in the S_n state, and ICs in the T_1 state were variable denoted as $[^3O_2]$, [S], and [T], respectively, and the following three kinetic equations, Equations (1), (2), and (3), were constructed.

$$\frac{d[^3O_2]}{dt} = -k_q[T][^3O_2] + k_o[^1O_2] = -k_q[T][^3O_2] + k_o([^3O_2]_0 - [^3O_2]) \quad (1)$$

$$\frac{d[T]}{dt} = k_{ISC}[S] - k_p[T] - k_{TS}[T] - k_q[T][^3O_2] \quad (2)$$

$$\frac{d[S]}{dt} = k_e[G] - k_{ISC}[S] - k_f[S] - k_{IC}[S] = k_e([I] - [S] - [T]) - [S](k_{ISC} - k_f - k_{IC}) \quad (3)$$

where […] represents the concentration of each species as follows. [G] represents the ICs in the S_0 state, [I] is the total concentration of ICs, [$^1O_2$] is the $^1O_2$ generated *via* the energy transfer from the T_1 of the ICs to $^3O_2$, and [$^3O_2$]$_0$ is $^3O_2$ in the initial state before UV irradiation. Parameter k_x is the rate constant of each process as follows: k_e for the photoexcitation process of the ICs from the S_0 to S_n state, k_{IC} for the internal conversion (non-radiative deactivation) from the S_n to S_0 state, k_f for the FL process, k_q for the OQ of the T_1 state *via* $^1O_2$ generation from $^3O_2$, and k_o for the transition from $^1O_2$ to $^3O_2$, where the k_o consists of three components *via* deactivation, exchange of $^3O_2$ between the inside and outside of the films, and consumption of oxygen *via* photodegradation of PMMA.

Each rate constant, k_x, was estimated from the measurements of the luminescence quantum yield and lifetime. Because k_e and k_o cannot be evaluated experimentally, they were treated as variable parameters and set that the order of magnitude of the simulated t_{ID} matches the values from the experimental results.

Fig. 9(a,b) compare the simulated and experimental results of the time evolution of the PIDL intensity during UV irradiation for ICs dispersed in PMMA. The simulated results successfully reproduced the experimental results, in which the PIDL emerged after an induction time, and the normalized intensities of the PIDL increased in the order of NT-IC<OD-IC<*s*BP-IC. Thus, the proposed mechanism of the PIDL is supported by a numerical simulation based on the hypothesized photophysical processes.

However, the slopes of the observed intensity curves from the onset of the PIDL deviate from those of the simulated curves. In the simulations, the rate constants were assumed to be unique values without spatial distributions and t_{ID} had no distribution, whereas k_o possibly varied depending on the depth in the film. The k_o value at the surface on the air side could be much larger than that inside the film because of the fast exchange of $^3O_2$ across the air surface of the films, while the k_o value near the substrate should be smaller because of the reduced exchange of $^3O_2$ by the restricted diffusion through the film.

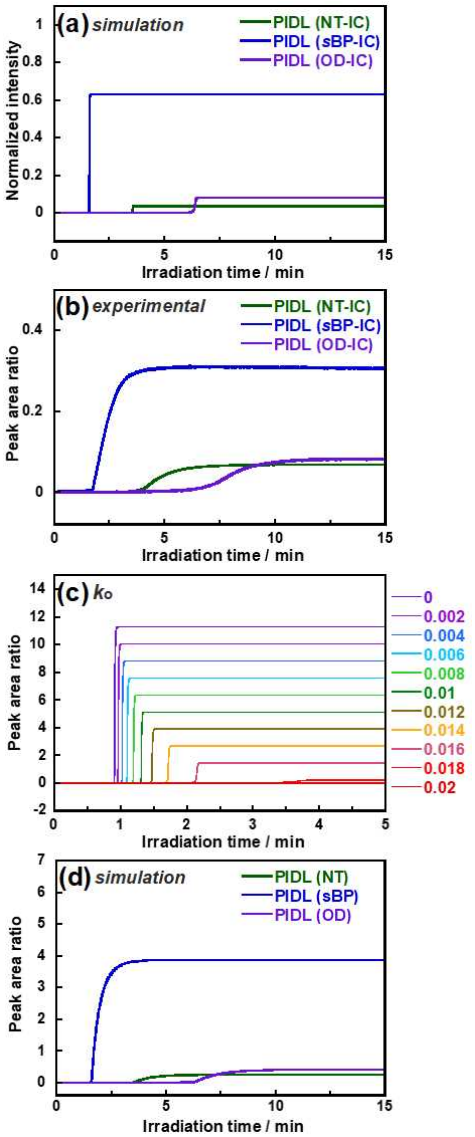

Fig. 9 Time evolution of the PIDL intensities of NT-IC, *s*BP-IC, and OD-IC dispersed in PMMA films of (a) simulated and (b) experimental data. (d) The sum of the PIDL intensity curves when k_o of ICs is varied in the (c) panel.

The simulated curves shown in **Fig. 9(c)** demonstrate that t_{ID} increases with k_o. **Fig. 9(d)** shows the PIDL curves, which are the sum of the respective PIDL intensities when k_o of NT-IC, *s*BP-IC, and OD-IC is varied in the range of 0.0061–0.0084 s^{-1}, 0.0061–0.0142 s^{-1}, and 0.0061–0.0069 s^{-1}, respectively. The summation curves of the calculated PIDLs emitted from ICs located at different depths by varying k_o and t_{ID} are closer to the observed PIDL curves, indicating that the PIDL increases more slowly with time compared with the simulated intensity without assuming the depth distribution of k_o.

4. Conclusion

An intriguing long-lived delayed-phosphorescence phenomenon, PIDL, was observed at room temperature in air for three ICs, NT-IC, *s*BP-IC, and OD-IC, dispersed in PMMA. The generation mechanism of the PIDL was investigated in detail by time-dependent luminescence measurements. These ICs exhibit only FL upon short-time UV irradiation in air, but after several minutes of continuous UV irradiation, that is, after a certain induction time, PIDL emerged and gradually increased, and a green afterglow lasted for several seconds after the irradiation was stopped. The induction time for the appearance of the PIDL is linearly proportional to [$^3O_2$] in air.

Based on the emission spectra measured during prolonged irradiation under various oxygen concentrations, the generation mechanism of PIDL was clarified as follows. $^3O_2$ around the ICs gradually decreased owing to the OQ of the ICs in the T_1 state, while the excited $^1O_2$ simultaneously increased. When most of the $^3O_2$ is consumed during irradiation, the rate constant of OQ significantly decreases and the ICs can exhibit PIDL. This mechanism is supported by the experimental results from the decrease in absorbance of DPBF, which is a probe to detect $^1O_2$, indicating that $^1O_2$ was generated by the OQ of ICs during UV irradiation. Finally, numerical simulations also supported the experimental results and revealed that the rate constant for $^1O_2$ deactivation in a polymer matrix (k_o) has a depth distribution from the surface of the films.

The results of this study demonstrate that the generation mechanism of the intriguing PIDL phenomenon is essentially based on the OQ of ICs dispersed in PMMA, which can be applied to the molecular design of new categories of room-temperature LL materials.

References

[1] I. B. Cohen, *Am Hist Rev* **1958**, *63*, 937.
[2] J. Botterman, P. F. Smet, *Opt Express* **2015**, *23*, A868.
[3] J. Xu, S. Tanabe, *J Lumin* **2019**, *205*, 581.
[4] J. Mei, Y. Huang, H. Tian, *ACS Appl Mater Interfaces* **2018**, *10*, 12217.
[5] X. Wang, H. Ma, M. Gu, C. Lin, N. Gan, Z. Xie, H. Wang, L. Bian, L. Fu, S. Cai, Z. Chi, W. Yao, Z. An, H. Shi, W. Huang, *Chemistry of Materials* **2019**, *31*, 5584.
[6] Y. Li, M. Gecevicius, J. Qiu, *Chem Soc Rev* **2016**, *45*, 2090.
[7] S. Mukherjee, P. Thilagar, *Chemical Communications* **2015**, *51*, 10988.
[8] P. Irmler, R. F. Winter, *Dalton Transactions* **2016**, *45*, 10420.
[9] K. Kanosue, S. Ando, *ACS Macro Lett* **2016**, *5*, 1301.
[10] K. Kanosue, S. Hirata, M. Vacha, R. Augulis, V. Gulbinas, R. Ishige, S. Ando, *Mater Chem Front* **2019**, *3*, 39.
[11] M. Doi, K. Muto, M. Nara, N. Liang, K. Sano, H. Mori, R. Ishige, S. Ando, *Journal of Photopolymer Science and Technology* **2021**, *34*, 423.
[12] Z. Mao, Z. Yang, Z. Fan, E. Ubba, W. Li, Y. Li, J. Zhao, Z. Yang, M. P. Aldred, Z. Chi, *Chem Sci* **2018**, *10*, 179.
[13] S. Tian, H. Ma, X. Wang, A. Lv, H. Shi, Y. Geng, J. Li, F. Liang, Z. Su, Z. An, W. Huang, *Angewandte Chemie* **2019**, *131*, 6717.
[14] E. Lucenti, A. Forni, C. Botta, L. Carlucci, C. Giannini, D. Marinotto, A. Previtali, S. Righetto, E. Cariati, *Journal of Physical Chemistry Letters* **2017**, *8*, 1894.
[15] Y. Xie, Y. Ge, Q. Peng, C. Li, Q. Li, Z. Li, *Advanced Materials* **2017**, *29*, 1606829.
[16] S. Hirata, M. Vacha, *Journal of Physical Chemistry Letters* **2016**, *7*, 1539.
[17] S. Hirata, K. Totani, J. Zhang, T. Yamashita, H. Kaji, S. R. Marder, T. Watanabe, C. Adachi, *Adv Funct Mater* **2013**, *23*, 3386.
[18] M. Doi, R. Ishige, S. Ando, **2023**, DOI: 10.1002/cptc.202200310.
[19] K. Narushima, Y. Kiyota, T. Mori, S. Hirata, M. Vacha, *Advanced Materials* **2019**, *31*, 1807268.
[20] Y. Su, S. Z. F. Phua, Y. Li, X. Zhou, D. Jana, G. Liu, W. Q. Lim, W. K. Ong, C. Yang, Y. Zhao, *Sci Adv* **2018**, *4*, eaas9732.
[21] N. J. Turro, V.Ramamurthy, J. C. Scaiano, *Modern Molecular Photochemistry of Organic Molecules*, University Science Books, **2010**.
[22] M. Gmelch, H. Thomas, F. Fries, S. Reineke, *Sci Adv* **2019**, *5*, eaau7310.
[23] M. Louis, H. Thomas, M. Gmelch, A. Haft, F. Fries, S. Reineke, *Advanced Materials* **2019**, *31*, 1807887.
[24] X. F. Zhang, X. Li, *J Lumin* **2011**, *131*, 2263.

[25] N. Harada, K. Masuda, J. ich Nakamura, H. Uyama, *Polym J* **2021**, *53*, 1383.
[26] N. Harada, M. Kataoka, M. Nakanosho, H. Uyama, *Photochem Photobiol* **2021**, *97*, 971.
[27] A. A. Krasnovsky, *J Photochem Photobiol A Chem* **2008**, *196*, 210.
[28] A. Blázquez-Castro, *Redox Biol* **2017**, *13*, 39.